FABRICATION OF THE ZnO NANOROD ARRAYS LED STRUCTURE GROWN ON *p*-TYPE GaN BY HYDROTHERMAL TECHNIQUE

Oleg Lupan, dr.Eng.
Technical University of Moldova

INTRODUCTION

The heterostructures of the *n*-ZnO nanorod arrays grown on the *p*-GaN were fabricated by a rapid hydrothermal technique. The grown ZnO nanorod arrays show a low density of intrinsic defect as demonstrated by Raman and photoluminescence studies. The characteristics of the heterojunction of the zinc oxide nanorod arrays with high crystalline quality deposited on *p*-GaN/Al$_2$O$_3$ substrate shows a rectifying behavior, a forward turn-on voltage of 4.4 V and a relatively high reverse current. The light emission investigations show that it can be proposed for further development to be used in nanodevice fabrication.

1. ZnO-NANOROD - BASED LIGHT EMITTING DIODES LEDs

ZnO and GaN are very attractive materials for researchers towards the development of optoelectronic devices in the blue and ultraviolet (UV) region. Previous studies on ZnO have revealed that such material is a promising one for exciton-based photonic devices in the UV region of spectra [1-4]. In the last few decades, the great development in single-crystal-growth technology by the epitaxial techniques has demonstrated the realization of blue and UV light-emitting devices, laser diodes, and photodetectors. Recently, ZnO nanorods on *p*-GaN substrates attracted much more interest due to nanosize – induced effects and possibility to develop higher efficiently and novel devices, e.g. single nanorod light source, etc.

ZnO films of high quality have been deposited on Al$_2$O$_3$, Si substrates by sophisticated techniques, like plasma assisted MBE [5-6]. However, it was observed the presence of degraded ZnO layer near to the interface region ZnO-substrate [5] due to a large lattice mismatch. Thus, the use of ZnO nanorod arrays and of substrates, like *p*-type GaN, with a small lattice mismatch (of

1.8%) would enhance the quality of material, especially close to interface region. Also, it is necessarily to mention a smaller thermal mismatch due to slight difference of coefficients of thermal expansion of ZnO and GaN. Thermal expansion coefficient are 6.51·10^{-6} and 5.59·10^{-6} (/°K) for ZnO and GaN, respectively [7]. Another important advantage of *n*-ZnO/*p*-GaN heterostructures would be the possibility to tune band line-up by controlling the interface bonds between ZnO and *p*-GaN as it is generally the case for heterovalent epitaxy [8]. Therefore, nano-ZnO/GaN heterojunctions have scientific interests and possibilities for making of novel devices based on it. Accordingly to multiple recent reports, ZnO nanorods and nanowires are becoming common building blocks for the next generation electronic devices [1-4]. However, for the achievement of its use in novel electronic, optoelectronic nanodevices there is a necessity in development of new fabrication tools for nanotechnology.

Here, it is necessarily to point out that there were only few reports on ZnO nanorods/*p*-GaN heterojunctions by relative low-temperature synthesis techniques [2,4]. Very recently, we investigated epitaxial growth of ZnO nanowires on *p*-GaN/Al$_2$O$_3$ substrates [2] by electrochemical deposition. Among these synthesis techniques, the hydrothermal process is very attractive as a simple and industrially economical method. Hydrothermal route has long been followed for growth of ZnO powder, single crystals [9]. However epitaxial growth of single crystalline ZnO nanostructures by hydrothermal method and latter integration in devices is yet to establish and there are only a few reports on this kind of research. Up to now, the integration of ZnO nanowires grown from solution phase in LED has not been very successful [10-12]. In previous reports a two steps approach is used, first the GaN is covered with a ZnO seed (which latter creates interface states) and the nanorods are subsequently grown from a zinc ion precursor solution. Until now, however, only visible light emitting LEDs (dominated by a violet-emission in Refs [10,12]) have been obtained by these

techniques. It is important to mention that such heterostructures needs the application of high voltages in the several tens of volts to observe the electro-emission. Also, some authors have pointed out the poor stability of the system and a decrease of light emission with increasing the diode current [10-12]. However, for consumer electronics it is of importance to develop stable LEDs which can work at lower applied voltage.

In this work, a rapid hydrothermal method was developed to synthesize *n*-ZnO nanorod arrays/*p*-GaN/sapphire heterostructure at low temperature (95-98°C) in 20 min and studied its characteristics. The high quality of the nanomaterial was demonstrated by micro-Raman and photoluminescence measurements. The corresponding heterojunction structures were integrated in efficient UV-LED structures.

2. EXPERIMENT DETAILS

Slices of a 1 μm thick Mg-doped GaN on *c*-Al_2O_3 (*p*-type GaN material) were used as a substrate for the fabrication of the ZnO nanorod arrays. GaN:Mg/Al_2O_3 substrates were initially degreased in an ultrasonic bath for 11 min sequentially in trichloroethylene, acetone, methanol, and deionized (DI) water, and then treated in concentrated HCl for 20 min to remove any native oxide. The samples were rinsed in DI water (electrical resistivity of 18.2 MΩ·cm) for 10 s and blown dry with nitrogen gas. In a typical procedure, samples was prepared using 0.1-0.5 M of zinc sulfate (99.5%) which was dissolved in 100 ml DI–water. An ammonia solution (NH_4OH) of 29.4% was added and solution was colorless. The vessels is placed on a preheated oven for 20 min at 96 °C and then allowed to cool down to room temperature for 40 min [13-14]. After the reaction was completed the grown ZnO nanorod arrays on the GaN substrates were rinsed in deionized water for 3 min and then the samples were dried in air at 170 °C for 10 min. Manipulation and reactions were inside a fume hood.

The samples with ZnO nanorods grown on GaN:Mg/Al_2O_3 substrates were studied by X-ray diffraction (XRD) using a Rigaku 'DB/MAX' powder diffractometer. The size and morphology of the samples with ZnO nanorods were observed with a scanning electron microscope (SEM). The composition of ZnO nanorods was carried out using the Energy dispersive X-ray spectroscopy (EDX), in combination with SEM. The room temperature Raman scattering was investigated with a Confocal Laser Raman System in the backscattering

geometry under the excitation by a 532 nm laser. Current-voltage (*I-V*) characteristics were measured using a semiconductor parameter analyzer with input impedance of 2.00×10^8 Ω [2-3].

3. RESULTS AND DISCUTIONS

The XRD scan shown in Figure 1 demonstrates that the ZnO nanorods grown on GaN substrate are with wurtzite structure. It can be seen that diffraction peaks at $2\theta=35.92$ and $2\theta=36.04$ are caused by crystalline (0002) ZnO with the hexagonal wurtzite structure (space group: P6$_3$*mc*(186); *a=b* = 0.3249 nm, *c* = 0.5206 nm) and wurtzite GaN (*a=b* = 0.3186 nm, *c* = 0.5178 nm), respectively. Lattice misfits between ZnO and GaN substrate for ZnO heteroepitaxy is 1.9%. The data are in agreement with the Joint Committee on Powder Diffraction Standards (JCPDS) card for zinc oxide (JCPDS 036-1451).
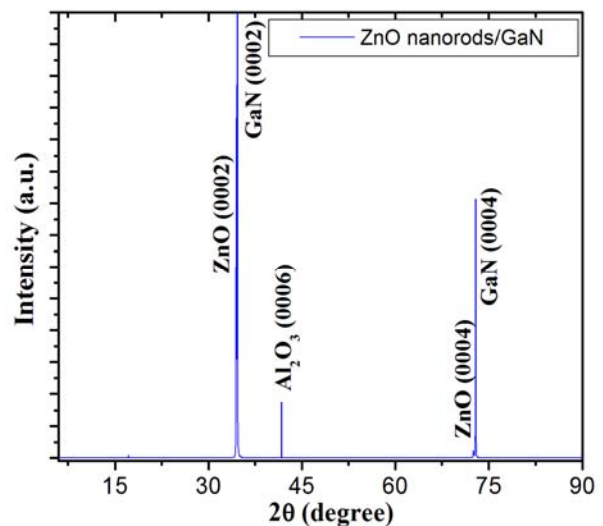

Figure 1. X-ray diffraction θ-2θ scan of the ZnO nanorods grown on GaN/sapphire (0001) substrate.

In investigated XRD pattern was observed the ZnO(0002) X-ray diffraction peak on the left-side of GaN(0002) reflection and the ZnO(0004) XRD peak on the left-side of the GaN(0004) reflection. All the patterns from our ZnO/GaN samples are typical of a perfectly textured ZnO material. The full width at half maximum (FWHM) of (0002) XRD peak for ZnO and GaN are low and similar at 0.10° and 0.08° respectively. Such values are typical of a high quality heterojunction. The *in-plane* alignment of the heterostructures was investigated by using XRD Φ scans (not shown). The *in-plane* epitaxial relationship in these heterostructures was found.
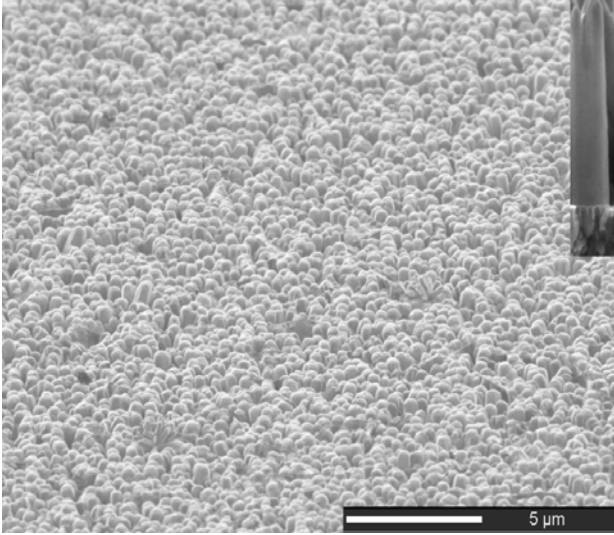
Figure 2. SEM image of ZnO nanorods hydrothermally grown on GaN substrate. Inset show cross-sectional SEM image of the ZnO nanorod/GaN hybrid structure grown on sapphire.

In order to examine the surface morphology SEM set-up has been used. Figure 2 shows SEM images of the ZnO nanorods hybrid structure grown on *p*-GaN layer. The high density of the zinc oxide nanorods was uniformly and oriented distributed on entire GaN surface. The number density of nanorods on surface was about 2×10^8 cm^{-2}. In case of lower synthesis temperature was observed growth of ZnO crystallites along the vertical and horizontal directions on the ZnO nanorods (not shown). The nanorods are free standing, grown vertically and are directly attached to the GaN thin film. Insert in Figure 2 shows cross-sectional SEM image of the ZnO nanorod/GaN hybrid structure grown on sapphire. Using energy dispersion X-ray spectroscopy, we found that the Zn:O ratios in our nanostructures to be 1:1 atomic ratio in all samples. The quality of the grown ZnO nanorods on GaN was found based on the stoichiometric composition deduced from the EDX analysis as well as by the XRD crystallographic data.

Further studies on the vibrational properties of ZnO nanomaterial are important in order to understand transport properties and phonon interaction with the free carriers, which latter determine device performance. In this order, the Raman spectrum (see Figure 3) of the ZnO nanorods on GaN was measured to get information about the material quality. The Raman spectrum was indexed with GaN and ZnO emission modes. The zinc oxide peaks are located at 100 cm^{-1} and 439 cm^{-1} and are attributed to the low- and high-E_2 mode respectively of non-polar optical phonons. The ZnO E_2(high) is clearly visible at 439 cm^{-1} with

a FWHM of 6 cm^{-1}, while the line-width of the peak corresponding to E_2(low) mode is about 3 cm^{-1}, which is comparable to values reported for high quality ZnO in the literature [2,4,15]. Since, the Raman spectrum investigations have been recorded with an incident light perpendicular to the top surface of the ZnO nanorod arrays on GaN substrate, then based on Raman selection rules the E_1(TO) and A_1(TO) modes are forbidden, when the incident light is parallel to the *c*-axis of nanorod arrays. In our studies, the absence of other phonon modes indicates that all nanorods are perpendicularly quasy-oriented to the substrate surface. It can be observed that ZnO nanorods are *c*-axis oriented, which is accordance with the SEM results presented above and XRD measurements.
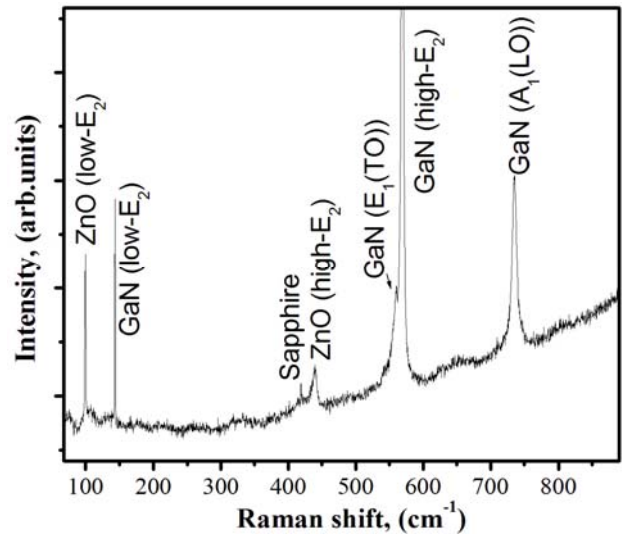

Figure 3. Room-temperature Raman spectra of ZnO nanorods hydrothermally grown on GaN substrate.

All Raman active modes can be observed in backscattering geometry. An exception is E_1(LO) mode, for which only the polarizability components involving *z* and the direction of phonon polarization change during vibration. Room-temperature Raman spectra of nanorods hydrothermally grown on GaN substrate demonstrates the high quality of the wurtzite crystal structure of our ZnO nanomaterial. Wurtzite ZnO belongs to the C_{6v} space group ($P6_3mc$). According to group theory, the corresponding zone centre optical phonons are of the following symmetry modes [13]:

$$\Gamma_{opt} = A_1 + 2B_1 + E_1 + 2E_2 \qquad (1)$$

The $A_1 + E_1 + 2E_2$ modes are Raman active and the $2B_1$ phonons are silent. The low-frequency E_2 mode is predominantly associated with the non-

polar vibration of the heavier Zn sublattice, while the high frequency E_2 mode involves predominantly the displacements of lighter oxygen atoms [15]. The A_1 and E_1 modes are split into longitudinal optical (LO) and transverse optical (TO) components. Except for the LO modes, all Raman active phonon modes are clearly identified in the measured spectrum (Figure 3).

Photoluminescence (PL) is a technique which can provide data related to deep-level (DL), and the ratio I_{UV}/I_{DL} (the intensity of the ultraviolet to the visible deep level related luminescence) is a measure of defect states in ZnO nanorods [3,15]. Accordingly to previous reports, typical zinc oxide exhibits an ultraviolet (UV) emission (at about 380 nm at room temperature) due to near band edge transitions [2,15]. The PL spectra of the near band-edge emission is dominated by the excitonic luminescence, while the emission related to the donor-acceptor pair recombination is around two orders of magnitude less intensive (Figure 4). The origin of the donor-acceptor luminescence band has been previously investigated in details [16-17].
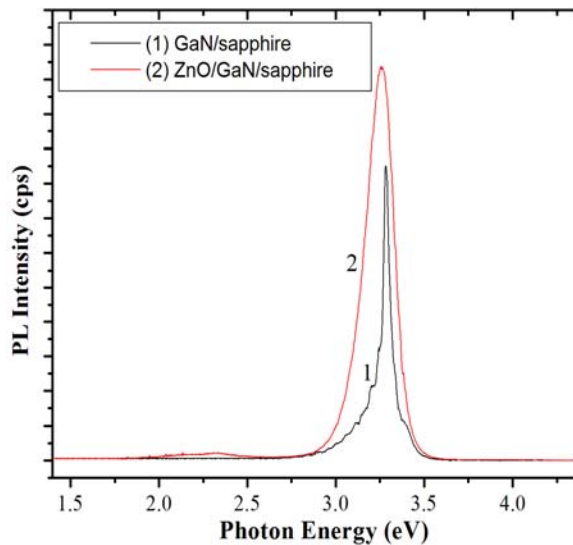
Figure 4. Photoluminescence spectra of the GaN/sapphire substrate (curve 1) and of the epitaxial ZnO-nanorods/p-GaN heterojunction (curve 2). Measurements were performed at 300 K.

Figure 4 shows the photoluminescence spectrum of the ZnO nanorod arrays hydrothermally gown and that of the GaN substrate investigated at room temperature. The GaN/sapphire spectrum posses only a single emission peak located at 3.29 eV and a FWHM of 11 nm. The ZnO spectrum indicates only a near band edge emission centered at 3.26 eV with a shoulder, which can be assigned to the GaN substrate emission.

4. *n*-ZnO/*p*-GaN HETEROJUNCTION INTEGRATED IN LED STRUCTURE

Figure 5 presents the cross-section schematic configuration of light-emitting diode structure based on the hydrothermally grown in 20 min ZnO-nanorods/p-GaN heterojunction. The top contact was made by using indium-tin oxide layer on glass, which is transparent to UV and visible light. The electrical contacts to p-GaN layer were made by using In-Ga eutectic. For more details see our recent reports [2,4].
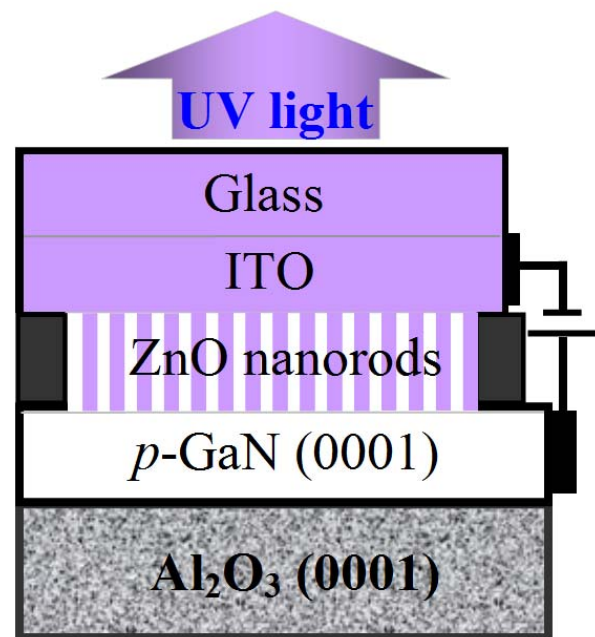
Figure 5. Schematic configuration of light-emitting diode structure based on the epitaxial ZnO-NRs/p-GaN heterojunction.

Figure 6 shows the current-voltage characteristics of the fabricated LED device structure measured in dark. It can be clearly seen that the ZnO nanorods forms a good rectifying heterojunction with the p-type GaN substrate. The *I-V* relation for a heterojunction can be described as follows:

$$I = I_s \left[\exp\left(\frac{qV}{kT} \right) - 1 \right] \qquad (2)$$

Where I is the current, q is the electronic charge, I_s is the saturation current, V is the applied potential across the ZnO/GaN heterojunction from p-GaN to n-ZnO nanorods side, k is the Boltzmann constant (1.38×10^{-23} J/K) and T is the absolute temperature. The rectifying behavior of fabricated heterojunctions can be seen in Figure 6 and the

turn-on voltage of about 4.4 V. These results clearly demonstrates that such kind of LED structures can work at lower voltages than previously reported ZnO nanowires on *p*-GaN structures with turn-on voltages higher than 10 V and currents >10 mA [10-12].
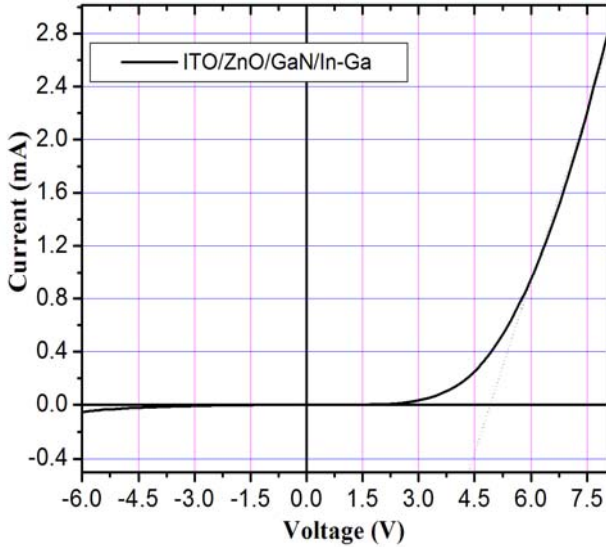

Figure 6. *I-V* characteristics of the ZnO nanorods/*p*-GaN heterojunction in the dark measured at 300 K.

Under a reverse bias, the *n*-ZnO/*p*-GaN heterojunction breaks down at about –7 V, and the leakage current reaches about 0.06 A. This could be due to defect-mediated tunneling effect caused by defect concentration or traps in the interfacial layer.
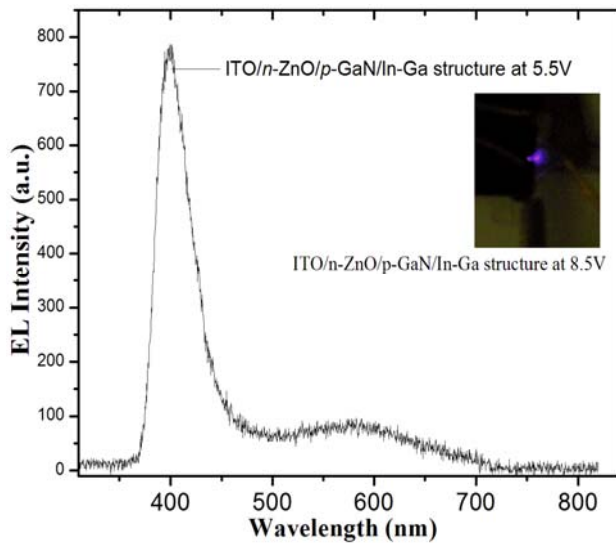

Figure 7. Electroluminescence characteristics of the epitaxial *n*-ZnO-nanorods/*p*-GaN heterojunction LED structure under -5.5 V forward bias. Insert shows image of the same structure under 8.5 V bias measured in the dark at 300 K.

Electroluminescence can be observed from *n*-ZnO nanorods/*p*-GaN LED structure at room temperature when a positive voltage is applied to the *p*-GaN/sapphire substrate accordingly to schematic representation from Figure 5. In our experiments no emission was observed under reverse bias of *p-n* heterojunction. Under forward bias of the structure presented in Figure 5, can be observed that UV emission dominates the electroluminescence spectra (see Figure 7).

To support discussions that the electroluminescence emission is from *n*-ZnO nanorods and *p*-GaN layer was drawn energy band diagrams based on Anderson model [18]. Energy band diagram of *n*-ZnO-nanorods/*p*-GaN heterojunction diode structure under the equilibrium state is presented in Figure 8.
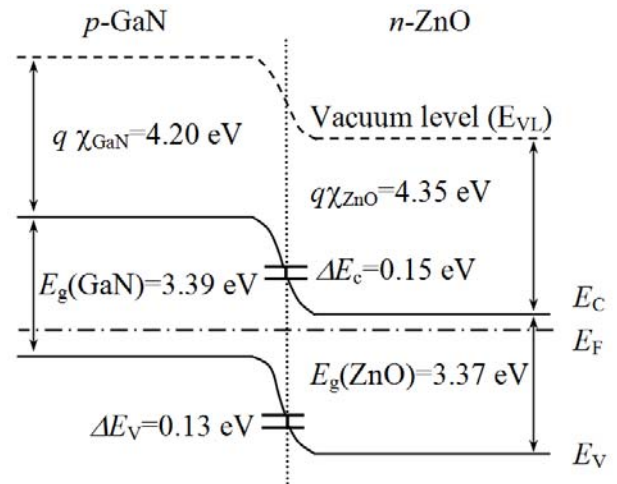

Figure 8. Anderson model energy-band diagram of the *n*-ZnO-nanorods/*p*-GaN heterojunction diode structure at thermal equilibrium.

Based on the diagram shown in Figure 8, the energetic barrier ΔE_c for electrons is:
$$\Delta E_C = q\chi_{ZnO} - q\chi_{GaN} = 4.35\,eV - 4.20\,eV = 0.15\,eV$$
and the energetic barrier for holes is:
$$\Delta E_V = E_g(ZnO) + \Delta Ec - E_g(GaN) =$$
$$= 3.37\,eV + 0.15\,eV - 3.39\,eV = 0.13\,eV$$
In such way can be concluded that the energy barrier for holes is close to the energy barrier for electrons in ZnO/GaN structures.

4. CONCLUSION

In summary, ZnO nanorod arrays on *p*-type GaN heterostructures were synthesized through a new and rapid hydrothermal route without template or seeds. The heterostructures are constructed of

high-quality ZnO nanorods confirmed by SEM, XRD, Raman and photoluminescence studies. These characterizations reveal that the ZnO material is composed from hexagonal faced one-dimensional nanorods with good crystal quality and *c*-axis orientation to GaN substrate.

The typical time taken to synthesize such *n*-ZnO-nanorods/*p*-GaN heterojunctions is 20 min. Also taken in the account that nanorod–based LED structures shows excellent rectifying and UV electroluminescence characteristics, we substantially contribute to overcome some obstacles in uses of nanorods/nanowires for LEDs production. Also have been satisfied the features of the nanowire synthesis method desired for industry are low-cost materials and processing, control of process parameters, environment friendly reagents, etc.

Further work: Our further research efforts are directed towards synthesizing oriented one – dimensional nanorods, which will facilitate construction of semiconductor nanodevices with well-ordered alignment, which are extremely important for scientific, technological and industrial application. Development of single doped ZnO nanorod LED for light emission sources.

References

1. M. Willander, L.L. Yang, A. Wadeasa, S.U. Ali, M.H. Asif, Q.X. Zhao, O. Nur, J. Mater. Chem. 19, p. 1006, 2009.

2. O. Lupan, T. Pauporté, B. Viana, I.M. Tiginyanu, V.V. Ursaki, R. Cortés, Epitaxial Electrodeposition of ZnO Nanowire Arrays on p-GaN for Efficient UV-Light Emitting Diode Fabrication. ACS Appl. Mater. Interfaces 2, p. 2083-2090, 2010.

3. I.M. Tiginyanu, O. Lupan, V.V. Ursaki, L. Chow, M. Enachi, Nanostructures of Metal Oxides. Comprehensive Semiconductor Science & Technology (SEST), Encyclopedia - edited by S. Wood, R. Fornari, and Hiroshi Kamimura, 2010.

4. O. Lupan, T. Pauporté, B. Viana, Low-voltage UV-Electroluminescence from ZnO-Nanowire Array/ p-GaN Light Emitting Diodes, Advanced Materials, 22, p. 3298-3302, 2010.

5. Y. Chen, J. Cryst. Growth, 181, p. 165, 1997.

6. Y. Chen, D.M. Bagnall, H.-J. Koh, K.-T. Park, K. Hiraga, Z.-Q. Zhu, T. Yao, J. Appl. Phys. 84, p. 3912, 1998.

7. R.D. Vispute, V. Talyansky, S. Choopun, R.P. Sharma, T. Venkatesan, M. He, X. Tang, J.B. Halpern, M.G. Spencer, Y. X. Li, L G. Salamanca-Riba, A.A. Iliadis, K.A. Jones, Appl. Phys. Lett., 73, n3, p. 348, 1998.

8. A. Franciosi, C.G. Van de Walle, Surf. Sci.Rep. 25, p. 1, 1996.

9. L.N. Demyanets, L.E. Li, T.G. Uvarova, Y.M. Mininzon, C.M. Briskina, O.M. Zhilicheva, S.V. Titkov, Inorg. Mater. 40, p. 1173, 2004.

10. S.D. Lee, Y.S. Kim, M.S. Yi, J.Y. Choi, S.M. Kim, J. Phys. Chem. C 113 p. 8954, 2009.

11. S. Kishwar, K. Hasan, G. Tzamalis, O. Nur, M. Willander, H.S. Kwack, D. Le Si Dang, Phys. Status Solidi (a) 207, p. 67, 2010.

12. A.M. Ng, Y.Y. Xi, Y.F. Hsu, A .B. Djurisic, W.K. Chan, S. Gwo, H.L. Tam, K.W. Cheah, H.F. Fong, H.F. Lui, C. Surya, Nanotechnology 20, p. 445201, 2009.

13. O. Lupan, L. Chow, G. Chai, B. Roldan, A. Naitabdi, A. Schulte, H. Heinrich, Nanofabrication and characterization of ZnO nanorod arrays, Materials Science and Engineering, B 145 p. 57, 2007.

14. O. Lupan, L. Chow, G. Chai, A. Schulte, S. Park, H. Heinrich, A rapid hydrothermal synthesis of rutile SnO$_2$ nanowires, Materials Science and Engineering, B 157 p. 101–104, 2009.

15. O. Lupan, V.V. Ursaki, G. Chai, L. Chow, G. Emelchenko, I.M. Tiginyanu, A.N. Gruzintsev, A.N. Redkin, Selective hydrogen gas nanosensor using individual ZnO nanowire with fast response at room temperature. Sensors and Actuators B: Chemical, 144, nr.1, p. 55-66, 2010.

16. V.V. Ursaki, I.M. Tiginyanu, V.V. Zalamai, V.M. Masalov, E.N. Samarov, G.A. Emelcenko, F. Briones, Photoluminescence of ZnO layers grown on opals by chemical deposition from zinc nitrate solution, Semiconductor Science and Technology, 19, p. 851-854, 2004.

17. V.V. Ursaki, O.I. Lupan, L. Chow, I.M. Tiginyanu, V.V. Zalamai, Rapid thermal annealing induced change of the mechanism of multiphonon resonant Raman scattering from ZnO nanorods, Solid State Communications, 143, p.437-441, 2007.

18. Ya.I. Alivov, E.V. Kalinina, A.E. Cherenkov, D.C. Look, B.M. Ataev, A.K. Omaev, M.V. Chukichev, D.M. Bagnall, Appl. Phys. Lett. 83, p. 4719, 2003.